

## Research paper

# Therapeutic effect of interstitial photodynamic therapy using ATX-S10(Na) and a diode laser on radio-resistant SCCVII tumors of C3H/He mice

S Nakajima, I Sakata,<sup>1</sup> T Hirano<sup>2</sup> and T Takemura<sup>3</sup>

Division of Surgical Operation, Asahikawa Medical College, Asahikawa 078, Japan. Tel: (+81) 166-69-3500; Fax: (+81) 166-65-6114. <sup>1</sup>Toyohakka Kogyo, Okayama 719-03, Japan. <sup>2</sup>Hamamatsu Photonics, Hamamatsu 431-31, Japan. <sup>3</sup>Research Institute for Electronic Science of Hokkaido University, Sapporo 060, Japan.

We examined the effect of interstitial photodynamic therapy (PDT) with a new photosensitizer ATX-S10(Na). This photosensitizer showed the strongest therapeutic effect 2-4 h after administration and was rapidly excreted from individual organs except tumor and liver 24 h after i.v. injection. Microscopic histofluorescent imaging showed fluorescence of ATX-S10(Na) in the cytoplasm of the tumor cells, but not in nuclei and in the vascular wall. Irradiation of Liniac 30 Gly+20 Gly slightly reduced the tumor size, but all mice died of relapse within 60 days after irradiation. In the PDT group, all tumors became non-palpable and healing was achieved in 50% of mice 120 days after PDT. [© 1998 Lippincott-Raven Publishers]

**Key words:** ATX-S10(Na), fluorescent tumor diagnosis, interstitial photodynamic therapy, photosensitizer, radio-resistant tumor.

## Introduction

In recent years, we have investigated new methods to diagnose and treat refractory advanced cancer using the tumor localizing capacity of porphyrin,<sup>1-5</sup> and we succeeded in developing a new photosensitizer, ATX-S10,<sup>6</sup> and a tumor tissue accumulating radiation sensitizer, KADTF.<sup>7</sup> In the present study, we performed interstitial photodynamic therapy (PDT) with a diode laser and ATX-S10(Na), which showed a stronger therapeutic photochemical effect than previously reported for ATX-S10. We examined whether indications for PDT, a local control for advanced cancer, could be expanded.

## Materials and methods

### Chemicals

We previously reported a new photo-chlorin photosensitizer ATX-S10<sup>6</sup> which was synthesized from protoporphyrin via photochemical reactions using the three-step process described by Sakata.<sup>8</sup> Recently, when the sodium salt of ATX-S10 was used to simplify the dissolution method, several derivatives that were conformational isomers were identified. Based on laboratory studies, the derivative with the structure shown in Figure 1 exhibited excellent tumor tissue uptake, and was therefore selected and designated ATX-S10(Na).<sup>9</sup> The chemical name of ATX-S10(Na) is 13, 17-bis (1-carboxypropionyl) carbamoyl ethyl - 8-ethenyl-2-hydroxy-3-hydroxyiminoethylidene-2,7,12,18-tetramethyl-porphine tetrasodium salt. Its molecular weight is 927.8. The longest wavelength absorbed by ATX-S10(Na) is 670 nm and the modulus of molar absorption is 16000, about five times that of photofrin injection (3000). The chemical structural formulae of ATX-S10 and ATX-S10(Na) are shown in Figure 1.

### Tumors

The tumor cell lines SCCVII, a squamous cell carcinoma implanted in C3H/He mice, was generously supplied by Dr Shibamoto (Kyoto University).<sup>7</sup> The tumor cells were maintained *in vitro* in Eagle's minimum essential medium (MEM) supplemented with 12.5% fetal bovine serum. All tumor cells were collected from a monolayer culture and approximately  $1.0 \times 10^5$  cells were inoculated s.c. in the right thigh of syngeneic female mice aged 8-11 weeks. Subcuta-

Correspondence to S Nakajima

neous tumors reaching 500–700 mm<sup>3</sup> after 12–14 days were used for experiments.

### Evaluation of the *in vitro* effects of PDT

HeLa cells were cultured in PRMI containing 10% fetal bovine serum. The culture medium was divided into microplates at a concentration of  $1 \times 10^6$  cells/ml. The microplates were mixed with previously reported ATX-S10 or ATX-S10(Na) to prepare concentrations of 5, 15, 25, 50 and 100  $\mu\text{M}/\text{cm}^3$ . Photoirradiation with an argon dye laser using a wavelength converted to 670 nm was administered at an intensity of 25 J/cm<sup>2</sup>. The photochemical tumoricidal effects of the two derivatives were evaluated based on the cell survival rate on Trypan blue staining.

### Biodistribution and tissue fluorescent diagnosis of ATX-S10(Na)

Biodistribution of ATX-S10(Na) was examined by N<sub>2</sub>-pulsed laser spectrofluorometry.<sup>1</sup> ATX-S10(Na) (15 mg/kg) was i.v. injected into SCCVII tumor-bearing C3H/He mice. The tumor and individual organs were removed 3, 6, 12 and 24 h after injection (three mice per time) to measure relative fluorescence intensity and tissue concentrations of ATX-S10(Na). ATX-S10(Na) for fluorescent diagnosis of tumors was evaluated using a tumor fluorescence imaging system developed at the Electronic Science Institute of Hokkaido University with a cooling type high-sensitivity CCD (Spectra Source Instruments, Westlake Village, USA). Each organ including the tumor of six mice (tumor, liver, lung, kidney, muscle and brain) was removed 3 h after i.v. injection of 15 mg/kg of ATX-S10(Na) into SCCVII tumor-transplanted C3H/He mice. Excited light (402 nm) was prepared using a mercury lamp and an interference filter. Red fluorescence of ATX-S10(Na) was photographed with a fluorescence image processing system (Fuji Film, Kanagawa, Japan).

### Fluorescence microscopic image

ATX-S10(Na) (15 mg/kg) was administered to six tumor-bearing mice. The SCCVII tumor was removed 3 h after injection of ATX-S10(Na). Frozen sections of each tumor embedded in OCT compound (Tissue-Tek, Miles Scientific, IL) were prepared for fluorescence microscopy (BX50-34-FLAD1; Olympus, Tokyo, Japan) coupled with a cooled CCD camera and an image processing system (Argus-50/C-CCD; Hamamatsu

Photonics, Hamamatsu, Japan) to estimate the location of the dye. A 5  $\mu\text{m}$  unstained frozen section was excited with 400–440 nm light and emission light through a dichromatic mirror (DM455; Olympus) and a 680 nm bandpass filter was detected with the CCD camera. Furthermore, frozen sections stained with hematoxylin & eosin were observed by light microscopy to facilitate precise localization of fluorescence.

### Laser and interstitial photoradiation system used in this experiment

A diode laser (Hamamatsu Photonics) was used for the *in vivo* PDT experiment. The laser was tuned to 670 nm for ATX-S10(Na) and the maximal output in this experiment was under 150 mW to avoid the effect of hyperthermia. A single quartz fiber interfaced to the laser was used to deliver light. To radiate light inside the tumor,<sup>10</sup> laser-proof polypropylene-based plastic tubing (external and internal diameter 1.5 and 1.2 mm, respectively, thickness 0.15 mm Yokohama Electronics Engineering Laboratory, Yokohama, Japan) was inserted into the tumor and an optic fiber was passed through the tube. The external and internal diameters of the optic fiber were 1.0 and 0.6 mm, respectively. The distal tip of the optic fiber was cut at an angle of 45° so that the laser beam was delivered perpendicularly to the axis of the optical fiber. As the plastic tubing was fabricated from scattering materials, the laser beam was emitted with scatter in a conical shape with large divergence (conical angle 33°). The fiber tip was rotated at a speed of 12 r.p.m. with a reciprocal motion from one end to the other at a speed of 18 mm/min. The radiation dose was expressed as the integrated energy emitted from 1 cm of tubing during one reciprocal motion of the fiber tip.

### Evaluation of the *in vivo* effects of PDT

When mean tumor diameter was 8–9 mm, 15 mg/kg of ATX-S10(Na) was i.v. injected into mice ( $n=6$ ). After 3 h, photochemical treatment was administered using a diode laser with wavelength of 670 nm (Hamamatsu Photonics) and a rotary tissue photoirradiation device.<sup>10</sup> Briefly, the fiber described above was inserted into the base of the tumor and photoirradiation was administered at an intensity of 90 J/cm under anesthesia with pentobarbital sodium (44 mM/kg). Two control groups were established; the untreated group ( $n=7$ ) and the radiotherapy group ( $n=7$ ) in which irradiation with 20 Gy was additionally administered using a Mitsubishi Liniac 15 MB2B irradiation device 7

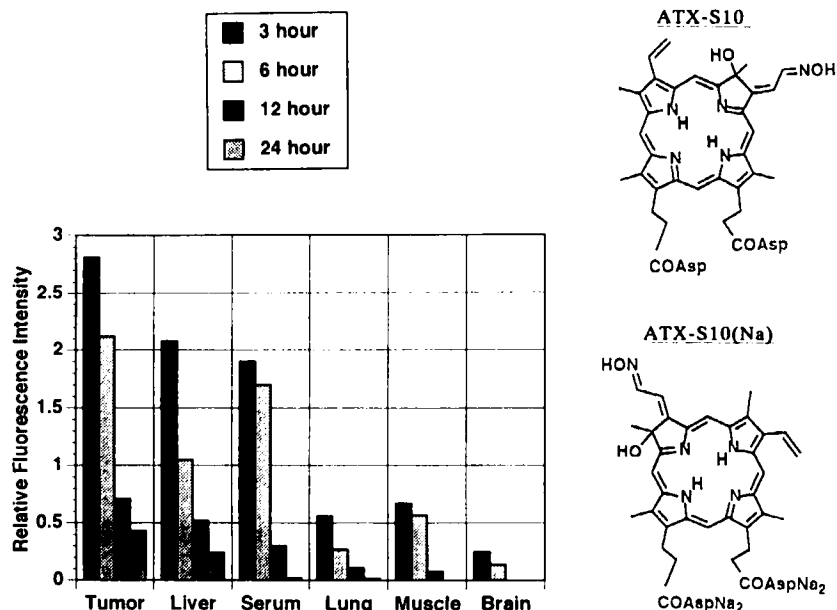


**Figure 1.** Chemical structure of ATX-S10 and ATX-S10(Na). *In vivo* distribution of ATX-S10(Na) measured by N<sub>2</sub>-pulsed laser spectrofluorometry. Vertical axis of this graph shows mean value of relative fluorescence intensity.<sup>1,2</sup>

days after irradiation with 30 Gly (total radiation dose 50 Gly). The tumoricidal activity of ATX-S10(Na) was determined by comparing the tumor growth curve and survival rate.

## Results

Figure 1 shows changes in ATX-S10(Na) concentrations in the tumor and each organ (tumor, liver, lung, muscle and brain) 3, 6, 12 and 24 h after 15 mg/kg of ATX-S10(Na) was i.v. injected into SCCVII tumor-transplanted C3H mice. As shown in the rod graph, ATX-S10(Na) accumulated in the tumor tissues early after administration, and was rapidly excreted from organs other than the tumor, liver and serum. Figure 2 shows the photochemical reaction-related tumoricidal effects of various concentrations of ATX-S10 and ATX-S10(Na) on cultured HeLa cells. ATX-S10(Na) had more potent tumoricidal effects than previously reported ATX-S10. Figure 3 shows fluorescence images of the tumor and each organ 3 h after injection of ATX-S10(Na). In the three mice, the strongest fluorescence of ATX-S10(Na) was detected in the tumor. ATX-S10(Na) may also be useful for tumor fluorescence diagnosis. Figure 4 shows fluorescence microscopic images of SCCVII tumor tissues. ATX-S10(Na) was accumulated in the cytoplasm of tumor cells excluding nuclei and in tumor vessels. Figure 5 shows the results

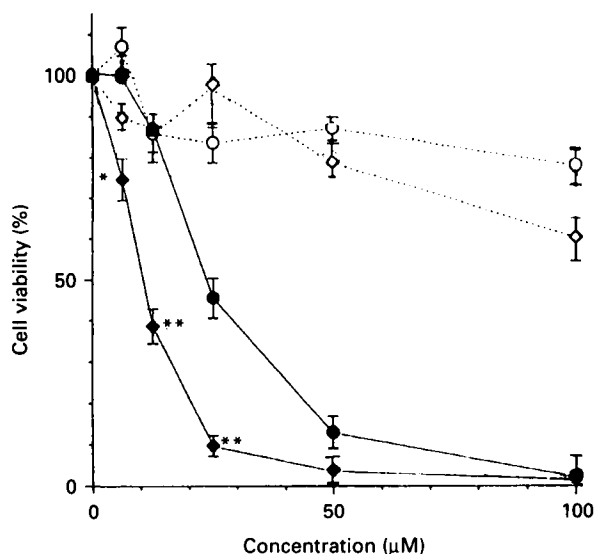


**Figure 2.** *In vitro* photodynamic tumoricidal effects of ATX-S10 and ATX-S10(Na). ○, ATX-S10 light(-); ●, ATX-S10 light(+); ◇, ATX-S10(Na) light(-); ◆, ATX-S10(Na) light(+).

of experimental interstitial PDT with a diode laser and a rotary tissue irradiation device after ATX-S10(Na) administration to SCCVII tumor-transplanted C3H mice. PDT group was significantly different from the non-treated group ( $p < 0.01$ ) and radiation group

( $p < 0.01$ ) in the change rate of the tumor volume. PDT with ATX-S10(Na) showed more potent tumoricidal effects than radiotherapy with 50 Gy of linac radiation. In addition, this radiotherapy did not induce healing in any animal. However, PDT administered once induced healing in 50% of mice. Figure 6 shows the survival curves for each therapy. In the group

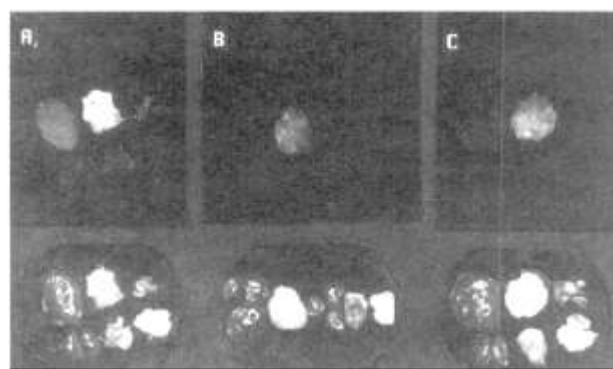


**Figure 3.** Upper row: fluorescence image. Lower row: image taken using a routine color CCD camera. Panels (A–C) show individual organs including the tumor of SCCVII tumor-transplanted C3H/He mice. (A) Upper row: liver, tumor and lung from the left. Lower row: Kidney, muscle and brain from the left. (B) From left to right: liver, tumor, lung, kidney, muscle and brain. (C) Same order as described in (A).

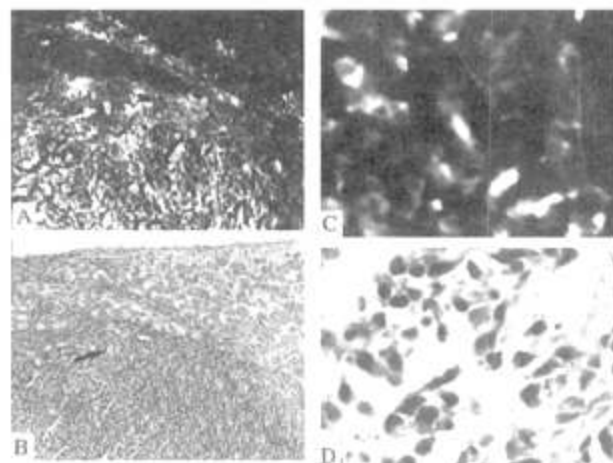


**Figure 4.** Fluorescence tissue image of the tumor 3 h after i.v. injection of ATX-S10(Na). (A) A fluorescence tissue image at 100-fold magnification. (B) The corresponding tissue image of (A) on hematoxylin & eosin (HE) staining. Arrows indicate tumor vessels. On the fluorescence image, the muscular region was 'black', while infiltrating tumor cells were white. (C) A fluorescence tissue image of the tumor site on the same section as (A) at 400-fold magnification. (D) The corresponding tissue image of HE staining.

treated by interstitial PDT, survival was significantly prolonged compared to that in the non-treated group ( $p < 0.05$ ). There was no significant difference between the radiation group and the non-treated group. Our data suggest that interstitial PDT with ATX-S10(Na) is more effective for local control of radio-resistant tumors such as SCCVII, than radiation alone treatment.

## Discussion

PDT is being used in clinical practice for treatment of various tumor types.<sup>11</sup> Recent studies have applied this therapy to early and advanced cancer

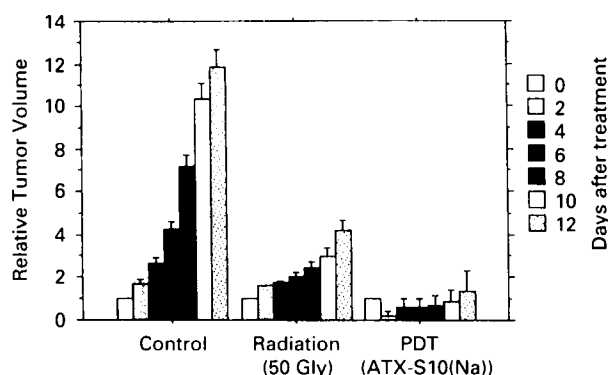


**Figure 5.** Inhibitory effects of the non-treated group (A) and irradiation of the 50 Gy group (B) and PDT following the ATX-S10(Na) administration group (C) on tumor proliferation (relative tumor volume ratio). There was a significant difference between group B and group C ( $p < 0.01$  by *t*-test).

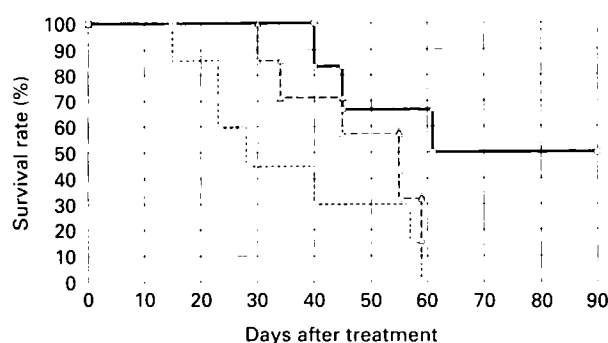


**Figure 6.** Survival curves of the non-treated and treated groups. Non-treated group (A), x; radiation group (B), Δ; PDT group (C), ○. There was a significant difference between the non-treated group (A) and PDT group (C) ( $p < 0.01$  by log-rank test).

treatments. Concerning photosensitizers, which are considered the most important, many kinds of agents have been synthesized, but these agents have limitations such as water solubility and prolonged retention *in vivo*. The development of effective and available photosensitizers is needed. ATX-S10(Na) which we developed is easily dissolved in distilled water for injection and has an absorption wavelength of 670 nm, demonstrating the lowest absorption of hemoglobin and water. This agent shows potent tumoricidal effects and is excreted from organs other than the tumor and liver within 24 h. Physicochemical characteristics did not differ between ATX-S10 previously reported<sup>6</sup> and ATX-S10(Na) investigated in this study, although there were differences in affinity for tumor tissues and selectivity. A slight change in the hydrophobicity of the R<sub>8</sub> side chain group may have caused the difference in biological effects between the two derivatives (unpublished data). The features of ATX-S10(Na) may overcome the limitations of Photofrin,<sup>12</sup> which showed a high complete response (CR) rate in patients with early lung cancer or cervical carcinoma in Japan. ATX-S10(Na) potently destroys cancer tissues despite rapid excretion. This may be associated with the vascular affinity of the chlorin derivative, as shown in fluorescence photographs (Figure 4) and as reported by Peng.<sup>13</sup> This feature should be efficiently utilized. In this experiment, we administered interstitial PDT to treat cancer.<sup>10</sup> This procedure expanded the indications for PDT from early stage cancer to large tumors. Interstitial PDT with ATX-S10(Na) did not adversely affect the whole body while showing potent tumoricidal effects. Furthermore, the use of a diode laser does not require any large expensive device. Therefore, this method may be a simple and effective form of cancer treatment. Furthermore, ATX-S10(Na) exhibits strong red fluorescence in tumor tissues and may be useful for tumor fluorescence diagnosis. Currently, we are also developing a radiation sensitizer, KADTF,<sup>7</sup> that accumulates in tumor tissue to establish a potent local cancer control method to be combined with interstitial PDT. ATX-S10(Na) has features that may also be useful for treating macular degeneration in the ophthalmological field. For clinical use, basic examination<sup>14</sup> is being performed.

## References

1. Nakajima S, Hayashi H, Omote Y, Yamazaki K, Maeda T. The tumor localizing properties of porphyrin derivatives. *J Photochem Photobiol* 1990; **7**: 189-98.
2. Nakajima S, Sakata I, Maeda T, Takemura T, Yamauchi Y, Koshimizu K. Detection and quantitative estimation of metalloporphyrins *in vivo*. *J Photochem Photobiol* 1991; **8**: 409-17.
3. Takemura T, Ohta S, Nakajima S, Sakata I. The mechanism of photosensitization in photodynamic therapy: phosphorescence behavior of porphyrin derivatives in saline solution containing human serum albumin. *Photochem Photobiol* 1991; **50**: 339-44.
4. Nakajima S, Yamauchi H, Sakata I, Yamazaki K, Maeda T, Takemura T. <sup>111</sup>In labeled Mn-metalloporphyrin for tumor imaging. *Nucl Med Biol* 1991; **20**: 231-7.
5. Nakajima S, Sakata I, Takemura T. Tumor-localizing activity of porphyrin and its affinity to LDL, transferrin. *Cancer Lett* 1995; **92**: 113-8.
6. Nakajima S, Sakata I, Takemura T, *et al*. Tumor-localizing and photosensitization of photo-chlorine ATX-S10. In: Spinelli P, Fante Dal, Marchesini R, eds. *Photodynamic therapy and biomedical lasers*. Amsterdam: Elsevier Science 1992: 531-4.
7. Nakajima S, Nishibe S, Murakami N, *et al*. Therapeutic and imaging capacity of tumor-localizing radiosensitive Mn-porphyrin on SCCVII tumor-bearing C3H/He mice. *Anti-Cancer Drugs* 1997; **8**: 386-90.
8. Sakata I, Inui Y, Maruyama I, Nakajima S, Takemura T. Synthesis and properties of ATX-S10 a analog. *Proc 16th Conf Japan Society for Laser Medicine* 1996; **16**: 161-8.
9. Nakajima S, Sakata I, Takemura T. Anti-tumor effect of second generation photosensitizer ATX-S10Na(II). *J Clin Exp Med (Igaku no Ayumi)* 1997; **189**: 689-90.
10. Hashimoto Y, Hirano T, Yamaguchi N. Novel after-loading interstitial photodynamic therapy of canine transmissible sarcoma with photofrin II and eximer dye laser. *Jpn J Cancer Res* 1995; **86**: 239-44.
11. Dougherty TJ. Photodynamic therapy. *Photochem Photobiol* 1995; **58**: 895-900.
12. Hayata Y, Kato H, Furuse K, Kusunoki Y, Suzuki S, Mimura S. Photodynamic therapy of 168 early stage cancer of the lung and esophagus: a Japanese multi-centers study. *Lasers Med Sci* 1996; **11**: 255-9.
13. Peng Q, Moan J, Ma L-W, Nesland JM. Uptake, localization, and photodynamic effect of meso-tetra(hydroxyphenyl) porphine and its corresponding chlorine in normal and tumor tissue of mice bearing mammary carcinoma. *Cancer Res* 1995; **55**: 2620-6.
14. Obana A, Gohto Y, Miki T, *et al*. Photodynamic therapy of choleoidal vessels using a newly-developed chlorin derivative (ATX-S10). *Proc Invest Ophthalmol Vis Sci* 1996; **37**: 5122.

(Received 10 March 1998; revised form accepted 23 April 1998)